scientific reports

OPEN

Antimicrobial activity of supramolecular salts of gallium(III) and proflavine and the intriguing case of a trioxalate complex

Marzia Guerrini[1], Simone d'Agostino[1], Fabrizia Grepioni[1], Dario Braga[1✉], Andrii Lekhan[2] & Raymond J. Turner[2✉]

The use of the gallium oxalate complex $[Ga(ox)_3]^{3-}$ as a building block in the formation of a drug-drug salt with the antimicrobial agent proflavine (PF) as its proflavinium cation (HPF^+), namely $[HPF]_3[Ga(ox)_3]\cdot 4H_2O$, is reported together with the preparation of the potassium salt $K_3[Ga(ox)_3]$ and the novel dimeric gallium(III) salt $K_4[Ga_2(ox)_4(\mu\text{-}OH)_2]\cdot 2H_2O$. All compounds have been characterized by solid state methods, and their performance as antimicrobial agents has been evaluated by disk diffusion assay against the bacteria strains *Pseudomonas aeruginosa* ATCC27853, *Staphylococcus aureus* ATCC25923, and *Escherichia coli* ATCC25922. While the $[HPF]_3[Ga(ox)_3]\cdot 4H_2O$ drug-drug salt is effective against all three strains, the gallium oxalate salt $K_3[Ga(ox)_3]$ showed impressive selectivity towards *P. aeruginosa*, with little to no antimicrobial activity against the other two organisms. This work presents novel breakthroughs towards Ga based antimicrobial agents.

An area of increasing interest is the possibility of obtaining new materials with competitive physico-chemical and pharmaceutical properties via a combined crystal engineering[1] and mechanochemical, solvent-free[2] approach. More specifically co-crystallization methods based on the direct reaction in the solid state (or in slurry conditions) have proven to be well suited for the preparation of new compounds in the solid form for subsequent applications and uses in a variety of fields[3,4].

One of these that is becoming increasingly important is that of microbe drug-resistance, i.e. the ability of bacteria to develop survival mechanism to evolve and protect themselves against the antimicrobial effect of pharmaceutical drugs, is increasingly affecting our ability to treat human and animal diseases[5–7]. Resistant microbes are difficult to treat leading us into the antimicrobial resistance (AMR) era[8]. Rather than increasing dosage, the possibility of finding alternative antimicrobial agents[9], natural bacterial killers, or novel drug formulations are key to resolving this challenge[10]. Further there is a need for controlling spread via bacterial growth on objects, surfaces, tools, etc[11]. This led us to ask, could using metal complexes, with known or potential antimicrobial activity paired with conventional organic antimicrobials a way to treat drug-resistant pathogens?

Our objective towards contributing to the quest for novel antimicrobials relies on an approach used successfully in previous occasions to prepare compounds possessing enzymatic inhibition capacity against enzymes such as amino-mono oxygenase and urease[12,13]. Essentially, this approach utilizes crystal engineering methods, such as the direct reaction between preformed molecular salts, to combine organic biocides with metal atom complexes that also possess antimicrobial properties. With this idea in mind we have already synthesized, structurally characterized, and subjected to antimicrobial assays a series of compounds where the biocide proflavine is co-crystallized together with Ag, Cu, and Zn salts or metal complexes[14,15], as all these metals exhibit strong antimicrobial activity[16,17].

Proflavine (see Fig. 1) is an established antimicrobial and is classified with the quaternary ammonium compounds (QCCs), which find use as antiseptics, cationic surfactants, disinfectants, herbicides, and dyes, with applications in domestic, clinical and industrial setting[18]. Proflavine antimicrobial mode of action is based on the

[1]Dipartimento di Chimica "Giacomo Ciamician", Università Di Bologna, Via Selmi, 2, 40126 Bologna, Italy. [2]Department of Biological Sciences, University of Calgary, 2500 University Drive NW, Calgary, AB T2N 1N4, Canada. ✉email: dario.braga@unibo.it; turnerr@ucalgary.ca
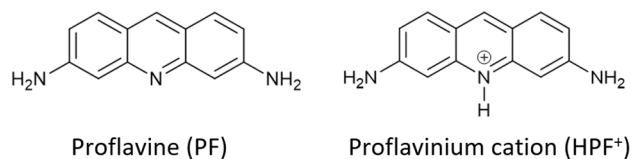
Figure 1. Neutral proflavine PF and monoprotonated proflavine, i.e. the proflavinium cation HPF+ used in this work.

intercalation between the nucleotide bases of DNA and further disrupting DNA replication and transcription[19]. Regions of DNA are also photosensitized upon intercalation and are subject to DNA strand breaks and point mutations[20].

In this paper we extend our approach to encompass a metal atom, gallium, whose antimicrobial properties have begun to be investigated in recent times[21,22]. Gallium, in its complexes and salts, is an emerging metal-based antimicrobials whose mechanism of action is based on Fe atom mimicry and thus interference with enzymatic processes dependent on Fe. Ga is competitively incorporated in Fe-containing metalloproteins but does not readily undergo redox reactions under the physiological conditions and therefore leaves the iron-dependent enzymes unfunctional[23]. Ga ions can easily get into bacterial cells by exploiting the Fe uptake system through replacing the Fe in iron savaging siderophores, which has led Ga to be referred to as a "Trojan horse" antimicrobial.

Hereafter we report on the preparation, structural characterization, and evaluation of the novel oxalate gallium complexes $K_3[Ga(ox)_3]\cdot3H_2O$ and $K_4[Ga_2(ox)_4(\mu\text{-OH})_2]\cdot2H_2O$ and of the proflavinium adduct $[HPF]_3[Ga(ox)_3]\cdot4H_2O$. The antimicrobial performance of these novel compounds against the bacteria strains *Pseudomonas aeruginosa* ATCC27853, *Staphylococcus aureus* ATCC25923, and *Escherichia coli* ATCC25922 using the established antimicrobial disk diffusion assay has been investigated and the results described in the following.

Materials and methods
All reagents and solvents were purchased from Sigma Aldrich and used without further purification.

Synthesis of $K_3[Ga(ox)_3]\cdot3H_2O$. *Solution synthesis* $Ga(NO_3)_3\cdot9H_2O$ (104.43 mg; 0.25 mmol) was dissolved in distilled water, and the solution was added to ca. 25 mL of an aqueous solution of $K_2C_2O_4\cdot H_2O$ (138.16 mg; 0.75 mmol). By addition of EtOH as antisolvent, a white suspension of $K_3[Ga(ox)_3]\cdot3H_2O$ was obtained, which was centrifuged and left to dry at ambient conditions. Single crystals of $K_3[Ga(ox)_3]\cdot3H_2O$ suitable for X-ray diffraction were grown in one week by vapour diffusion of EtOH into an aqueous solution containing $Ga(NO_3)_3\cdot9H_2O$ and $K_2C_2O_4\cdot H_2O$ in 1:3 stoichiometric ratio. *Solid state synthesis* $K_3[Ga(ox)_3]\cdot3H_2O$ could also be obtained in the solid-state, either by manual grinding in agata or porcelain mortar and via mechanical milling with a Retsch MM200 Mixer Mill. In this last procedure, the same quantities of solid reagents used for the solution synthesis were added to a 5 mL agate jar containing 2 balls of 5 mm diameter; the solid mixture was milled for 1 h, yielding a white fine powder of $K_3[Ga(ox)_3]\cdot3H_2O$ (see SI for X-ray characterization).

Synthesis of $K_4[Ga_2(ox)_4(\mu\text{-OH})_2]\cdot2H_2O$. A serendipitous result was obtained when a 1:3 stoichiometric mixture of $Ga(NO_3)_3\cdot9H_2O$ (104.43 mg; 0.25 mmol) and $K_2C_2O_4\cdot H_2O$ (138.16 mg, 0.75 mmol) was dissolved in water, and acetone vapours were let to diffuse into the solution (vapor diffusion technique): at the aqueous solution/acetone interface single crystals formed in a matter of days, which were characterized via X-ray diffraction as the salt $K_4[Ga_2(ox)_4(\mu\text{-OH})_2]\cdot2H_2O$, containing the dimeric gallium(III) anion $[Ga_2(ox)_4(\mu\text{-OH})_2]^{4-}$ (see SI for a comparison of the X-ray experimental pattern and the one calculated on the basis of single crystal data).

Synthesis of [HPF]Cl. Commercial $[HPF]_2[SO_4]\cdot xH_2O$ (1 g) was dissolved in 25 mL of water and NaOH (3.10 g, 0.077 mol) was added to the solution, yielding $PF\cdot H_2O$[24,25] as a crystalline powder. $PF\cdot H_2O$ was then dissolved in an equimolar quantity of HCl 0.1 M under stirring at ambient conditions. The chloride salt was recovered after solvent evaporation, and its XRPD pattern compared with the one calculated from single crystal data[26].

Synthesis of $[HPF]_3[Ga(ox)_3]\cdot4H_2O$. A 3:1 stoichiometric mixture of $PF\cdot HCl\cdot2H_2O$ (281.708 mg, 1 mmol) and $K_3[Ga(ox)_3]\cdot3H_2O$ (168.38 mg, 0.33 mmol) was dissolved in 35 mL of water; the solution was heated to 70 °C and left under stirring for 24 h. Upon solvent evaporation dark red crystals suitable for X-ray diffraction were obtained, which were filtered and left to dry at ambient conditions.

Powder X-Ray diffraction. For phase identification purposes room temperature X-ray diffraction patterns were collected on a PANalytical X'Pert PRO automated diffractometer equipped with an X'celerator detector in the 2θ range 3°–40° (step size 0.0167, time/step 50 s, VxA 40×40).

Single crystal X-ray diffraction. Single Crystal data for all compounds were collected at room temperature with an Oxford Diffraction X´Calibur equipped with a graphite monochromator and a CCD detector. Mo-Kα radiation (λ = 0.71073 Å) was used. Relevant crystal data and details of measurements are listed in Table S1. The structure was solved by the Intrinsic Phasing methods and refined by least squares methods against F^2 using SHELXT-2016[27] and SHELXL-2018[28] with Olex2 interface[29]. Non-hydrogen atoms were refined

anisotropically. H_{CH} atoms were added in calculated positions; H_{OH} and H_{NH} atoms were either located from a Fourier map or added in calculated positions and refined riding on their respective carbon, nitrogen, or oxygen atoms. One proflavinium cation was found to be disordered ca. 50:50 over two positions. Mercury 4.3[30] was used for graphical representations and for powder patterns simulation on the basis of single crystal data. Crystal data can be obtained free of charge from the Cambridge Crystallographic Data Centre via https://www.ccdc.cam.ac.uk and have been allocated the accession numbers CCDC 2123788-2123789.

Thermogravimetric analysis (TGA). TGA measurements were performed using a Perkin-Elmer TGA7 under an N_2 gas flow, at a heating rate of 5 °C min^{-1}.

Hot stage and cross polarized optical microscopy (HS-CPOM). For a thermal characterization of the samples a Linkam TMS94 device, connected to a Linkam LTS350 platinum plate and supplied with polarizing filters, was used. The imaging software VisiCam Analyzer, from an Olympus BX41 stereomicroscope, was simultaneously employed.

Antimicrobial activity. Antimicrobial efficacy was assessed as in previous work[14,15] according to current disk diffusion susceptibility testing protocols[31]. *Pseudomonas aeruginosa* ATCC27853, *Staphylococcus aureus* ATCC25923, *Escherichia coli* ATCC25922 indicator strains were used in this study. All culturing was performed in Lysogeny Broth (LB) prepared in distilled water with 10 g/L NaCl (VWR International Co., Mississauga, Canada), 5 g/L yeast extract (EMD Chemicals Inc., Darmstadt, Germany) and 10 g/L tryptone (VWR Chemicals LLC, Solon, USA). Agar medium for disk diffusion assays was obtained by adding 15 g/L bacteriological agar (VWR International LLC, Solon, USA) to the above-mentioned LB. In an aseptic environment, 200 μl of overnight culture of *S. aureus*, *P. aeruginosa* or *E. coli* was spread on LB agar plates (2 plates per organism for two technical replicates) and left to dry at room temperature for 1 h. Stocks of 24 mg/mL stock solutions of single components and suspensions/slurries of target crystal compounds were prepared from powder using the LB media. Six antimicrobial disks (Oxoid Ltd, Basingstoke, UK) were placed into a vial with 300 μL of compound stocks (AgNO₃, proflavine, and test compounds) and left to soak for 30 min with mixing every 10 min by inversion of the vial. Then disks were transferred to the plates (total of 2 replicates per compound per organism) and plates incubated at 37 °C for 24 h. The zone of growth inhibition was measured by a ruler. For one to see a zone of inhibition, the compounds need to release from the filter disk and diffuse through the LB-agar media a consequence of which gives a concentration gradient. Biocidal versus inhibitory effect was established by touching the inhibited growth zone with a microbiological loop and streaking to a fresh agar plate, if the growth appeared in this plate, the compound was considered bacteriostatic, if no growth was present, the compound was considered bactericidal. The ability of the compound to kill pre-formed bacterial lawn was performed as follows. In aseptic environment, 200 μL of overnight culture of *S. aureus*, *P. aeruginosa* or *E. coli* was spread on LB agar plates (2 plates per organism for replicates) and cultivated overnight to receive the bacterial lawn. Antimicrobial disks used for previously described disk diffusion assay were removed from the previous plate with sterile tweezers and placed upside-down on the plates with the pre-formed bacterial lawn. Plates were then left overnight at 37 °C and disks removed from the plates with sterile tweezers. Zones under the disks were then assessed for bacterial lysis.

Results and discussion

Before discussing the antimicrobial activity, it is worth examining the molecular and crystal structures of the three novel compounds $K_3[Ga(ox)_3]\cdot 3H_2O$, $K_4[Ga_2(ox)_4(\mu\text{-}OH)_2]\cdot 2H_2O$ and of the proflavinium adduct $[HPF]_3[Ga(ox)_3]\cdot 4H_2O$ (see Fig. 2).

The trianion $[Ga(ox)_3]^{3-}$ in the salt $K_3[Ga(ox)_3]\cdot 3H_2O$ is isostructural with octahedral oxalate complexes of di- and trivalent metals, such as zinc(II), chromium(III), iron(III), aluminum(III), among others. The three oxalate dianions act as bidentate ligands towards gallium(III); the oxygen atoms not involved in the coordination to gallium interact in turn with the potassium cation. The first coordination sphere around the potassium cation is completed by water molecules that occupy channels extending along the crystallographic *c*-axis (see Fig. 3, left) and interacting via hydrogen bonds with the oxalate anions. TGA measurements (see Fig. S5) show the loss of only one water molecule per formula unit, most likely the one evidenced in azure in Fig. 3 (right), i.e. the water molecule located in the inner part of the channel.

The structure of $K_4[Ga_2(ox)_4(\mu\text{-}OH)_2]\cdot 2H_2O$ is shown in Fig. 4. Each gallium(III) belonging to the dimeric anion is coordinated by two oxalate dianions and two bridging hydroxyl groups, with the six oxygen atoms describing a distorted octahedron around the metal centre. Ga-O_{OH} distances, in the range 1.929(6)–1.957(6) Å, are in line with the bond lengths found in the Cambridge Structural Database for related compounds.

The structure of the proflavinium adduct $[HPF]_3[Ga(ox)_3]\cdot 4H_2O$ is shown in Fig. 5 (left). It is noteworthy that the proflavinium cations form stacks around the gallium tris oxalate core, in such a way as to completely envelope the anion. Figure 5 (right) shows the layered arrangement of the cations and the location of the water molecules, mostly arranged in layers parallel to the *b*-axis.

TGA measurement on $[HPF]_3[Ga(ox)_3]\cdot 4H_2O$ shows a loss of ca. 7% of the total molecular weight (see Fig. S6). Since the mass loss corresponds approximately to the percentage of water contained in the hydrated compound, it is likely due to complete dehydration. This process was also investigated via HSM. Single crystals of $[HPF]_3[Ga(ox)_3]\cdot 4H_2O$ were immersed in oil and heated at 10 °C min^{-1} from RT to 120 °C; the loss of water could be visually observed in the form of gaseous water bubbles starting at ca. 75 °C (see Fig. S7). The dehydration process is reversible: variable temperature X-ray diffraction on powder (see Fig. S8) shows a different pattern for the anhydrous compound at 120 °C, but on going back to room temperature the water molecules are captured
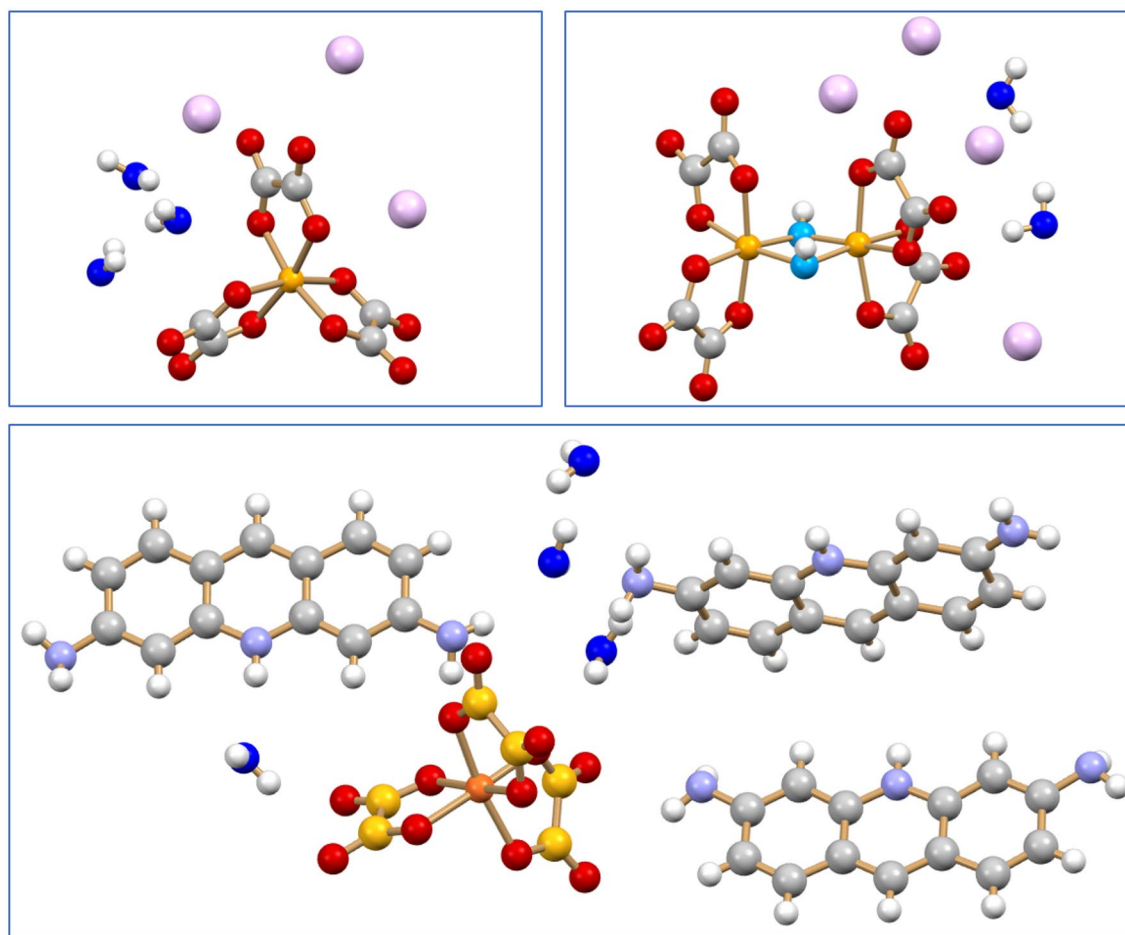
Figure 2. Schematic representation of the three compounds described in this work: $K_3[Ga(ox)_3] \cdot 3H_2O$ (top left), $K_4[Ga_2(ox)_4(\mu\text{-}OH)_2] \cdot 2H_2O$ (top right) and the proflavinium adduct $[HPF]_3[Ga(ox)_3] \cdot 4H_2O$ (bottom). [K^+ in violet, O_W atoms in blue, C_{OX} in light orange in the proflavinium adduct].
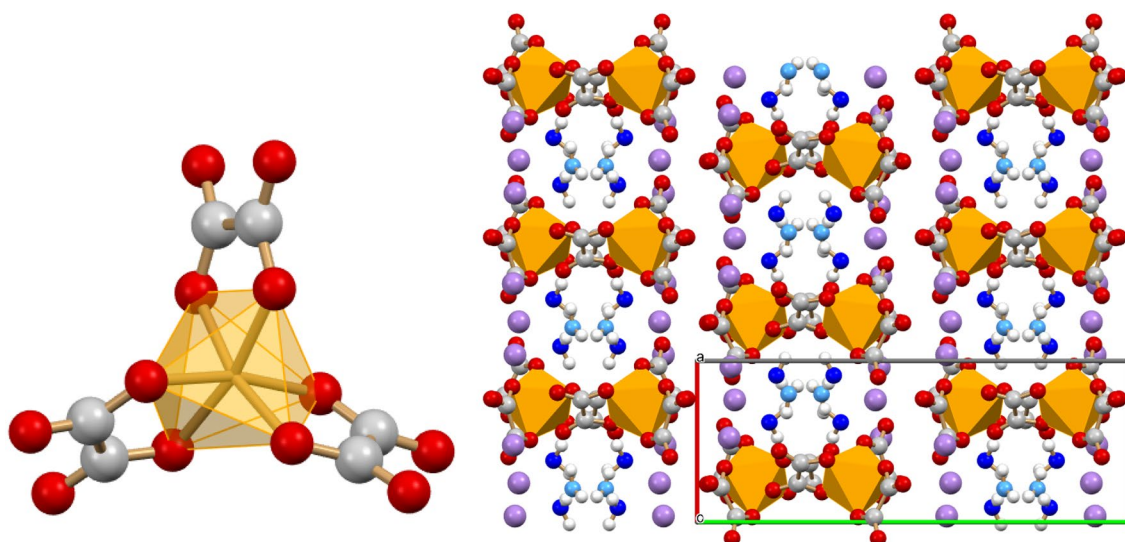
Figure 3. (Left) The structure of the $[Ga(ox)_3]^{3-}$ complex; (right) the channels accommodating the water molecules in the crystal structure of $K_3[Ga(ox)_3] \cdot 3H_2O$. K^+ in violet, O_W atoms in blue and cyano.
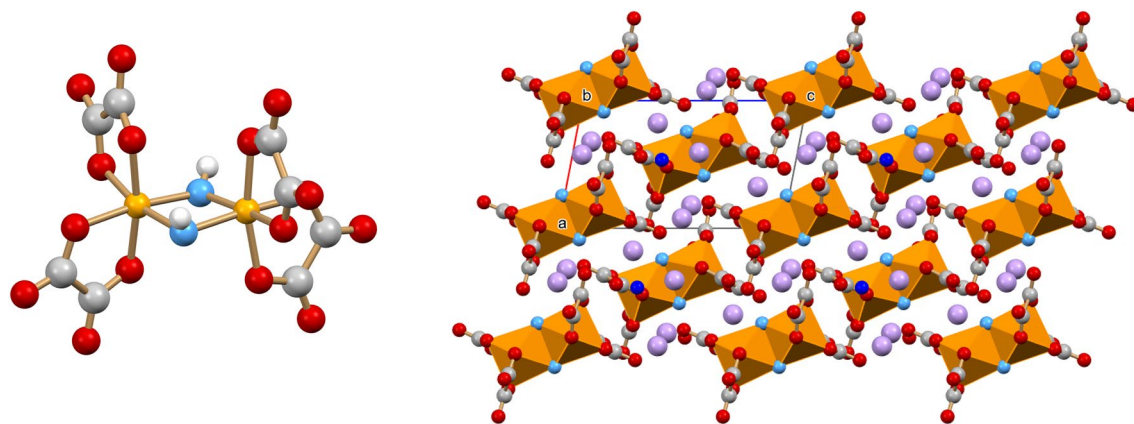
Figure 4. (Left) The $[Ga_2(ox)_4(\mu\text{-}OH)_2]^{4-}$ dimeric anion showing the bridging OH groups; (right) the packing arrangement viewed along the b-axis in crystalline $K_4[Ga_2(ox)_4(\mu\text{-}OH)_2]\cdot2H_2O$. K^+ in violet, O_W in blue, O_{OH} in cyano; H atoms omitted for clarity.
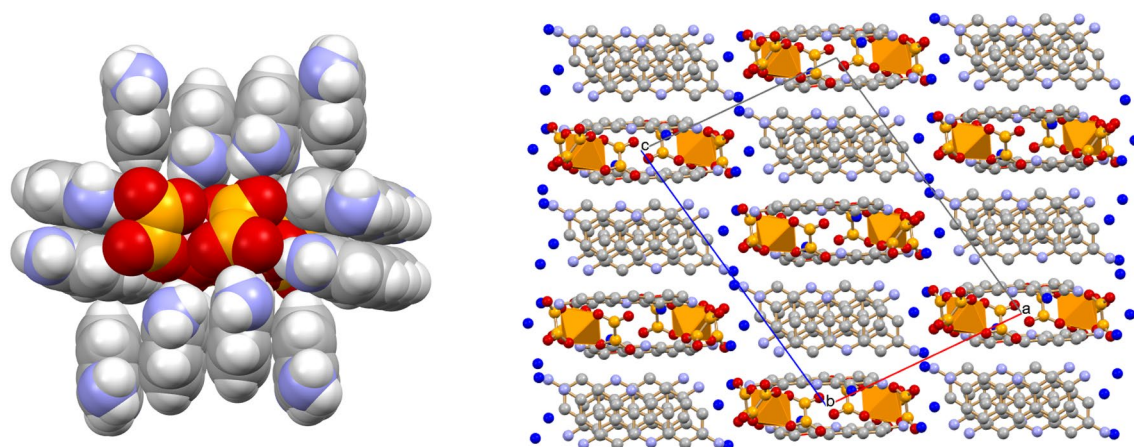
Figure 5. (Left) The proflavinium cations enveloping the $[Ga(ox)_3]^{3-}$ anions in crystalline $[HPF]_3[Ga(ox)_3]\cdot4H_2O$; (right) the packing in crystalline $[HPF]_3[Ga(ox)_3]\cdot4H_2O$ viewed along the crystallographic b-axis. O_W in blue; H atoms omitted for clarity.

again, and the crystalline material recovered at the end of the heating–cooling cycle is the hydrated compound $[HPF]_3[Ga(ox)_3]\cdot4H_2O$.

Antimicrobial assays

As found previously[32–34], differences in antimicrobial susceptibility towards metal-based antimicrobials is seen between the three different strains. The strains chosen for evaluation include a Gram-negative enteric pathogen *Escherichia coli,* the opportunistic pathogen and ubiquitous soil organism *Pseudomonas aeruginosa* and the Gram-positive opportunistic pathogen *Staphylococcus aureus.* All three of these organisms are listed by World Health Organization as priority pathogens (*P. aeruginosa* and *E. coli*—critical priority, *S. aureus*—high priority), for which development of new antimicrobials is critically important[35].

Antimicrobial activity was evaluated using the established antimicrobial disk zone[36,37] of inhibition assay which has been used to explore similar proflavine–metal cocrystals[14,15]. Here we compare the zone of growth inhibition of bacterial strains spread on LB agar plates to that of silver nitrate. Silver is the most popular metal based antimicrobial[38] and thus serves well to compare new metal based antimicrobial formulations to. Additionally, ratioing to the internal standard controls for plate-to-plate variations. Here, in Fig. 6, a value > 1 is more effective than silver and a value < 1 is less antimicrobial than silver.

We see that proflavine on its own has strong antimicrobial activity against all three strains, slightly greater than silver. $K_3[Ga(ox)_3]\cdot3H_2O$ and $K_4[Ga_2(ox)_4(\mu\text{-}OH)_2]\cdot2H_2O$ behaved very similarly, showing efficacy only against *P. aeruginosa.* There was no visible zone of inhibition against either *E. coli* or *S. aureus.* It is somewhat remarkable to observe such selectivity of this formulation of Ga towards only the *Pseudomonas*, particularly since we see that $Ga(NO_3)_3$, which provides Ga^{3+} ions to enter via the Trojan horse mechanism, has activity slightly less than that of silver nitrate to all three organisms, as supported elsewhere[39]. In order to inflict toxicity to bacteria, Ga must be taken into the cell to replace Fe in proteins. The explanation likely originates through the difference of metallophore/siderophore acquisition systems for cellular iron uptake. *P. aeruginosa* primary system is through the *Pseudomonas* specific siderophore, pyoverdine[40]. Whereas *E. coli* uses a variety of diverse systems[41], and *S. aureus*
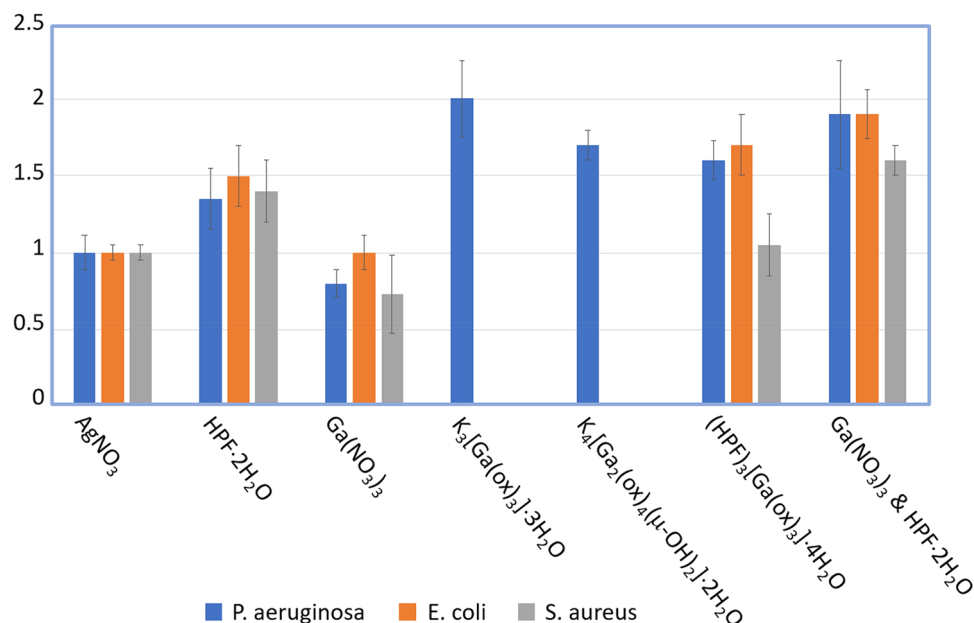
Figure 6. Antimicrobial efficacy of gallium compounds in comparison with proflavine and silver nitrate. The bars represent antimicrobial zone of inhibition assay where data are normalized to zone of $AgNO_3$. The last set of columns on the right denotes effectiveness of combining the gallium nitrate salt with proflavine in solution both at 24 mg/mL, thus at higher molar load, and is designated by the '&' notation. Data shows error deviations between trials. (n = 2–6 trials).

tends to take Fe from heme[42]. We can posit a hypothesis that the complex and dynamic structure of pyoverdine (consisting of a dihydroxyquinoline core, a 6–14 amino acid variable sequence peptide and a α-keto acid derived from the Krebs cycle) has the ability to coordinate the Ga-oxalate complex or outcompete the oxalate ligands for the Ga atom. Such dynamic metallophores are not produced by the other two bacteria. This reflects the different lifestyles and ecological niches of the investigated bacterial strains that leads to different siderophores available and thus differently evolved receptors and transporters[43].

The $[HPF]_3[Ga(ox)_3] \cdot 4H_2O$ proflavine-gallium adduct showed efficacy against all three strains. The efficacy against *S. aureus* was the same as that of silver, but less than proflavine, but the combination worked well against the other two pathogens. To be noted, the co-crystal gave superior antimicrobial performance towards *E. coli* and *P. aeruginosa* essentially 50% better than proflavine alone. Here it suggests the presence of the gallium led to enhancement of proflavine toxicity to *E. coli*. To compare the crystal formulation, we loaded disks with a mixture of $Ga(NO_3)_3$ and HPF proflavine each at 24 mg/mL (last column set in Fig. 6). It required this very high load of antimicrobial mix to get to the same antimicrobial efficacy (within experimental variance) as the proflavine-gallium co-crystal ($[HPF]_3[Ga(ox)_3] \cdot 4H_2O$, second last column in Fig. 6). If we consider the molar composition of the co-crystals, they contain less gallium and proflavine molecules per unit mass, thus their antimicrobial activity is likely much more superior than what is illustrated by the outcome presented in Fig. 6.

At this time, one can only provide conjectures to the mechanism of action of this drug-drug crystal. We can hypothesize that cell contact with the crystalline material induces changes in the physicochemical environment, leading to crystal decomposition on the cell surface. This would then provide a very high local dose of each of HPF and Ga ions for a devastating local ambush.

Assessment of contact killing properties of the compounds showed that all the novel compounds were able to lyse *E. coli* and *S. aureus* pre-grown lawn of cells upon overnight exposure, while the pre-grown *P. aeruginosa* cells were able to withstand the contact with the antimicrobial-soaked disks. This suggests that $[HPF]_3[Ga(ox)_3] \cdot 4H_2O$, $K_3[Ga(ox)_3] \cdot 3H_2O$ and $K_4[Ga_2(ox)_4(\mu\text{-OH})_2] \cdot 2H_2O$ possess bactericidal properties with regard to *E. coli* and *S. aureus* but are bacteriostatic against *P. aeruginosa* in regard to a contact assay compared to the results of Fig. 6 where compounds are evaluated to inhibit growth.

Conclusions

Metal-based antimicrobials have been gaining popularity as a new means to deal with the increasing antimicrobial resistance. The challenge is substantial and calls for the exploration of novel approaches and of novel antimicrobial agents. Gallium has not been as extensively explored as other metals in terms of antimicrobial activity per se and in conjunction with other molecules known to performance against common bacteria strains. In this paper we have reported the synthesis, structural characterization and antimicrobial performance of novel coordination compounds of gallium(III), namely the trianion $[Ga(ox)_3]^{3-}$ and the dimeric tetraanion $[Ga_2(ox)_4(\mu\text{-OH})_2]^{4-}$ as their hydrated K^+ salts, and we have utilized the trianion $[Ga(ox)_3]^{3-}$ in the preparation of a co-crystal by reaction with the solid hydrochloride salt of the proflavinium cation HPF^+. The product is a novel supramolecular salt

containing three proflavinium cations in the form of the hydrated salt $[HPF]_3[Ga(ox)_3]\cdot 4H_2O$. This latter compound has also been subjected to antimicrobial assay against ATCC pathogen indicator strains of *P. aeruginosa*, *S. aureus* and *E. coli*, and has been shown to be effective against all three strains, thus behaving as a drug-drug salt. This study also highlights specificity of gallium ligated species uptake between the three bacteria strains, with only *P. aeruginosa* able to recognize and uptake the gallium oxalate species.

References

1. Desiraju, G. R. Crystal Engineering: A holistic view. *Angew. Chem. Int. Ed.* **46**, 8342–8356 (2007).
2. James, S. L. *et al.* Mechanochemistry: Opportunities for new and cleaner synthesis. *Chem. Soc. Rev.* **41**, 413–447 (2012).
3. Wouters, J. & Quéré, L. *Pharmaceutical Salts and Co-crystals* (Royal Society of Chemistry, 2011).
4. Gopi, S. P., Ganguly, S. & Desiraju, G. R. A drug-drug salt hydrate of norfloxacin and sulfathiazole: Enhancement of in vitro biological properties via improved physicochemical properties. *Mol. Pharm.* **13**, 3590–3594 (2016).
5. Levy, S. B. & Bonnie, M. Antibacterial resistance worldwide: Causes, challenges and responses. *Nat. Med.* **10**, S122–S129 (2004).
6. Brown, E. D. & Wright, G. D. Antibacterial drug discovery in the resistance era. *Nature* **529**, 336–343 (2016).
7. Streicher, L. M. Exploring the future of infectious disease treatment in a post-antibiotic era: A comparative review of alternative therapeutics. *J. Glob. Antimicrob. Resist.* **24**, 285–295 (2021).
8. Ferri, M., Ranucci, E., Romagnoli, P. & Giaccone, V. Antimicrobial resistance: A global emerging threat to public health systems. *Crit. Rev. Food Sci. Nutr.* **57**, 2857–2876 (2017).
9. Kargar, F. *et al.* Binuclear Zn(II) Schiff base complexes: Synthesis, spectral characterization, theoretical studies and antimicrobial investigations. *Inorg. Chim. Acta* **530**, 120677 (2022).
10. Ghosh, C., Sarkar, P., Issa, R. & Haldar, J. Alternatives to conventional antibiotics in the era of antimicrobial resistance. *Trends Microbiol.* **4**, 323–338 (2019).
11. Thabit, A. K., Crandon, J. L. & Nicolau, D. P. Antimicrobial resistance: Impact on clinical and economic outcomes and the need for new antimicrobials. *Expert Opin. Pharmacother.* **16**, 159–177 (2015).
12. Casali, L. *et al.* Novel dual-action plant fertilizer and urease inhibitor: The urea·catechol co-crystal—characterization and environmental reactivity. *ACS Sustain. Chem. Eng.* **7**, 2852–2859 (2019).
13. Mazzei, L. *et al.* Multifunctional urea cocrystal with combined ureolysis and nitrification inhibiting capabilities for enhanced nitrogen management. *ACS Sustain. Chem. Eng.* **7**, 13369–13378 (2019).
14. Fiore, C., Shemchuk, O., Grepioni, F., Turner, R. J. & Braga, D. Proflavine and zinc chloride "team chemistry": Combining antibacterial agents via solid-state interaction. *CrystEngComm* **23**(25), 4494–4499 (2021).
15. Shemchuk, O., Braga, D., Grepioni, F. & Turner, R. J. Co-crystallization of antibacterials with inorganic salts: Paving the way to activity enhancement. *RSC Adv.* **10**, 2146–2149 (2020).
16. Turner, R. J. Metal-based antimicrobial strategies. *Microb. Biotechnol.* **10**, 1062–1065 (2017).
17. Lemire, J. A., Harrison, J. J. & Turner, R. J. Antimicrobial activity of metals: Mechanisms, molecular targets and applications. *Nat. Rev. Microbiol.* **11**, 371–384 (2013).
18. Wainwright, M. Acridine: A neglected antibacterial chromophore. *J. Antimicrob. Chemother.* **47**, 1–13 (2001).
19. Hurwitz, J., Furth, J., Malamy, M. & Alexander, M. The role of deoxyribonucleic acid in ribonucleic acid synthesis. III. The inhibition of the enzymatic synthesis of ribonucleic acid and deoxyribonucleic acid by actinomycin D and proflavin. *Proc. Natl. Acad. Sci. USA* **48**, 1222–1230 (1962).
20. Piette, J. *et al.* Visible-light-induced OH radicals in DNA-proflavine Complexes: An e.p.r and spin trapping study. *Int. J. Radiat. Biol. Relat. Stud. Phys. Chem. Med.* **42**, 151–161 (1982).
21. Hijazi, S. *et al.* Antimicrobial activity of gallium compounds on ESKAPE pathogens. *Front. Cell Infect. Microbiol.* **8**, 316 (2018).
22. Gugala, N., Chatfield-Reed, K., Turner, R. J. & Chua, G. Using a chemical genetic screen to enhance our understanding of the antimicrobial properties of gallium against *Escherichia coli*. *Genes (Basel)* **10**, 34 (2019).
23. Bernstein, L. R. Mechanisms of therapeutic activity for gallium. *Pharmacol. Rev.* **50**, 665–682 (1998).
24. Neidle, S. & Jones, T. A. Crystal structure of proflavine, a DNA binding agent. *Nature* **253**, 284–285 (1975).
25. Achari, A. & Neidle, S. Nucleic acid binding drugs. Proflavine free base. *Acta Crystallogr. Sect. B* **32**, 2537–2539 (1976).
26. Obendorf, S. K., Carrell, H. L. & Glusker, J. P. *Acta Crystallogr. Sect. B Struct. Crystallogr. Cryst. Chem.* **30**, 1408–1411 (1974).
27. Sheldrick, G. M. Integrated space-group and crystal-structure determination. *Acta Crystallogr Sect. A* **71**, 3–8 (2015).
28. Sheldrick, G. M. Crystal structure refinement with SHELXL. *Acta Crystallogr. Sect. C* **71**, 3–8 (2015).
29. Dolomanov, O. V., Bourhis, L. J., Gildea, R. J., Howard, J. A. K. & Puschmann, H. OLEX2: A complete structure solution, refinement and analysis program. *J. Appl. Crystallogr.* **42**, 339–341 (2009).
30. MacRae, C. F. *et al.* Mercury 4.0: From visualization to analysis, design and prediction. *J. Appl. Crystallogr.* **53**, 226–235 (2020).
31. Balouiri, M., Sadiki, M. & Ibnsouda, S. K. Methods for *in vitro* evaluating antimicrobial activity: A review. *J. Pharm. Anal.* **6**, 71–79 (2016).
32. Gugala, N., Lemire, J. J. & Turner, R. J. The efficacy of different anti-microbial metals at preventing the formation of, and eradicating bacterial biofilms of pathogenic indicator strains. *J. Antibiot.* **70**, 775–780 (2017).
33. Gugala, N., Vu, D., Parkins, M. D. & Turner, R. J. Specificity in the susceptibilities of *Escherichia coli, Pseudomonas aeruginosa*, and *Staphylococcus aureus* clinical isolates to six metal antimicrobials. *Antibiotics.* **8**, 51 (2019).
34. Pormohammad, A. & Turner, R. J. Silver antibacterial synergism activities with eight other metal(loid)-based antimicrobials against *Escherichia coli, Pseudomonas aeruginosa*, and *Staphylococcus aureus*. *Antibiotics.* **9**, 853 (2020).
35. World Health Organization. *Global Priority List of Antibiotic-Resistant Bacteria to Guide Research, Discovery, and Development of New Antibiotics*: https://www.who.int/medicines/publications/WHO-PPL-Short_Summary_25Feb-ET_NM_WHO.pdf.
36. CLSI. *Performance Standards for Antimicrobial Disk Susceptibility Tests, Approved Standard. CLSI document M02–A11* 7th edn. (Clinical and Laboratory Standards Institute, 2012).
37. Jan, H. *Kirby-Bauer Disk Diffusion Susceptibility Test Protocol* (American Society for Microbiology, European Committee On Antimicrobial Susceptibility Testing, 2009). "EUCAST disk diffusion method": https://www.eucast.org/fileadmin/src/media/PDFs/EUCAST_files/Disk_test_documents/2021_manuals/Manual_v_9.0_EUCAST_Disk_Test_2021.pdf
38. Lansdown, A. B. Silver in health care: Antimicrobial effects and safety in use. *Curr. Probl. Dermatol.* **33**, 17–34 (2006).
39. Gugala, N., Vu, D., Parkins, M. D. & Turner, R. J. Specificity in the susceptibilities of *Escherichia coli, Pseudomonas aeruginosa*, and *Staphylococcus aureus* clinical isolates to six metal antimicrobials. *Antibiotics* **8**, 51 (2019).
40. Bonneau, A., Roche, B. & Schalk, I. J. Iron acquisition in Pseudomonas aeruginosa by the siderophore pyoverdine: An intricate interacting network including periplasmic and membrane proteins. *Sci. Rep.* **10**, 120 (2020).
41. Braun, V. Iron uptake by *Escherichia coli*. *Front. Biosci.* **8**, 1409–1421 (2003).

42. Mazmanian, S. K. *et al.* Passage of heme-iron across the envelope of *Staphylococcus aureus*. *Science* **299**, 906–909 (2003).
43. Krewulak, K. D. & Vogel, H. J. Structural biology of bacterial iron uptake. *Biochim. Biophys. Acta* **1778**, 1781–1804 (2008).

Acknowledgements

Author contributions

Competing interests

The authors declare no competing interests.

Additional information

Supplementary Information The online version contains supplementary material available at https://doi.org/10.1038/s41598-022-07813-0.

Correspondence and requests for materials should be addressed to D.B. or R.J.T.

Reprints and permissions information is available at www.nature.com/reprints.

Publisher's note Springer Nature remains neutral with regard to jurisdictional claims in published maps and institutional affiliations.